THE JOURNAL OF PHYSICAL CHEMISTRY LETTERS
A JOURNAL OF THE AMERICAN CHEMICAL SOCIETY

pubs.acs.org/JPCL

Letter

How Heterogeneity Affects Cooperative Communications within Single Nanocatalysts

Bhawakshi Punia, Srabanti Chaudhury,*,∇ and Anatoly Kolomeisky*,∇

Cite This: J. Phys. Chem. Lett. 2023, 14, 8227−8234

Read Online

ACCESS | Metrics & More | Article Recommendations | Supporting Information

ABSTRACT: Catalysis remains one of the most essential methods in chemical research and industry. Recent experiments have discovered an unusual phenomenon of catalytic cooperativity, when a reaction at one active site can stimulate reactions at neighboring sites within single nanoparticles. While theoretical analysis established that the transport of charged holes is responsible for this phenomenon, it does not account for inhomogeneity in the structural and dynamic properties of single nanocatalysts. Here, we investigate the effect of heterogeneity on catalytic communications by extending a discrete-state stochastic framework to random distributions of the transition rates. Our explicit calculations of spatial and temporal properties of heterogeneous systems in comparison with homogeneous systems predict that the strength of cooperativity increases, while the communication lifetimes and distances decrease. Monte Carlo computer simulations support theoretical calculations, and microscopic arguments to explain these observations are also presented. Our theoretical analysis clarifies some important aspects of molecular mechanisms of catalytic processes.

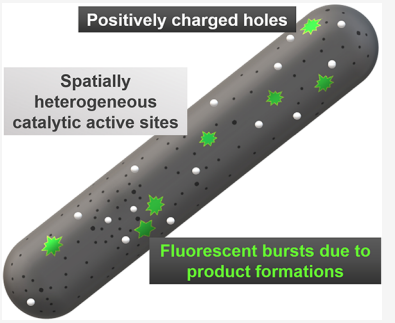

Rates of chemical reactions are governed by the highest energetic barriers on the path to breaking old bonds and creating new ones. Catalysis is a powerful method of accelerating these chemical reactions by adding certain compounds that are not consumed in these reactions, called catalysts, that provide alternative faster free-energy pathways.[1] From living systems to industrial processes, catalytic phenomena have been extensively studied over the years, but the underlying microscopic mechanisms in many systems have not been fully clarified.[2,3] In particular, there are multiple questions to understand heterogeneous catalysis where the reactants, catalysts, and products might exist in distinct thermodynamic phases.[4−6]

Recent advances in nanotechnology have led to the development of various types of nanoparticles as promising heterogeneous catalysts with potentially wide applications.[7,8] Nanocatalysts might be synthesized in specific shapes and sizes that help to rationally tune their catalytic properties, increasing their efficiency.[9−11] Another advantage of nanoparticles is that catalytic processes can now be investigated with high temporal and spatial resolution, uncovering phenomena that could not be observed in bulk-solution experiments.[12−18] One of the most surprising recent observations obtained using single-molecule fluorescence microscopy is a discovery of catalytic communications between surface active sites in gold (Au) and palladium (Pd) nanoparticles.[19] Analysis of correlations between successive time-dependent product formation events occurring at different segments of nanoparticles revealed that chemical reactions at specific sites effectively stimulate chemical reactions at the neighboring sites but the effect weakens with the distance and time. Such correlations might exist up to ∼10−100 s and the corresponding correlation lengths are reaching ∼200−600 nm.[19] These experiments also indicated that charged holes are most probably responsible for this phenomenon.

Single-particle experimental measurements found that the rates of product formation and product dissociation on nanocatalysts show a wide range of distribution, indicating the existence of strong temporal fluctuations at the molecular level. Furthermore, these nanoparticles might undergo dynamic restructuring, exhibiting different chemical activity with changes in size.[20−22] Several experiments have also demonstrated changes in the catalytic efficiency of the nanocatalysts, depending on their facet shapes.[23−25] These spatiotemporal fluctuations might be also connected with surface defects on nanoparticles that can disturb the arrangement of active sites on the lattice.[26,27] As a result, the catalytic reactivity patterns might differ significantly between apparently similar nanoparticles.[26] These findings indicate that nanocatalysts are strongly heterogeneous systems, and this should affect their catalytic properties.

To explain the microscopic mechanisms of catalytic communications in single nanoparticles, we recently proposed a novel discrete-state stochastic framework to study catalysis of

Received: July 8, 2023
Accepted: September 1, 2023
Published: September 6, 2023

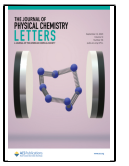

https://doi.org/10.1021/acs.jpclett.3c01874
J. Phys. Chem. Lett. 2023, 14, 8227−8234

redox chemical reactions.[28] Single-molecule microscopy experiments have reported both intraparticle and interparticle communications in catalytic reactions on Pd- or Au-based nanocatalysts through redox processes.[19] As experimental evidence suggest that a positively charged species is responsible for cooperative catalytic communication within single nanocatalysts by moving along oxide surfaces of nanoparticles, it was assumed that the probability for a chemical reaction to occur at the given site depends on the local concentration of positively charged holes,[29−31] and each chemical reaction also creates new charged holes. The idea was that the increased local concentration of charged holes forces them to move into the areas of the nanoparticle with smaller concentrations, and this stimulates chemical reactions at neighboring sites due to incoming charged particles increasing the concentrations of charged holes around these sites.[28] A quantitative model based on these ideas has been developed, allowing for explicit estimates of communication lifetimes and distances. Excellent agreement with all available experimental observations has been found. Importantly, this theoretical approach was able to explain not only the characteristic spatial and temporal lengths scales of catalytic communications and their dependence on external electric fields but also the universality and robustness of this phenomenon.[28] At the same time, this theoretical approach neglected a crucial aspect of heterogeneity of nanoparticles,[24−27,32,33] raising an important question of how inhomogeneous microscopic rates that control the dynamics of charged particles will affect the catalytic communications phenomenon in single nanoparticles.

In this paper, we present a theoretical investigation of the role of heterogeneity in catalytic communications within single nanoparticles. By extending the original homogeneous stochastic approach to a more realistic heterogeneous description, we evaluated the cooperativity in catalyzed chemical reactions on the single nanoparticle, using explicit calculations and Monte Carlo computer simulations. By specifically considering several heterogeneous distributions of transition rates that spatially vary along the nanoparticles, communication lifetimes, and correlation lengths are evaluated. Our analytical calculations and computer simulations indicate that heterogeneity increases the strength of correlations while catalytic communication distances and lifetimes generally decrease. Theoretical arguments to explain these observations are also presented.

Let us analyze catalytic cooperativity processes in a single nanoparticle, as shown in Figure 1a. Since experiments were mostly performed on nanorods, in our analysis, we also concentrate only on one-dimensional (1D) nanocatalysts.[19] The single nanorod particle can be viewed as a lattice consisting of multiple segments, and each segment is assumed to have a length l(in nanometers), similar to what was done in the analysis of single-molecule fluorescent measurements of catalyzed chemical reactions.[19] The number of active sites in each segment might vary, reflecting the heterogeneity of the system (Figure 1a). It is assumed also that only one type of redox chemical reaction can take place on any active site of the nanocatalyst. In addition, since these reactions involve charged species such as electrons and holes, we postulate that the probability of a chemical reaction occurring at the specific site depends on the local concentration of charged holes, and each reaction creates a new charged hole with a rate k (Figure 1a). The charged holes can diffuse along the nanorod with equal probability in both directions, and the migration rate out of

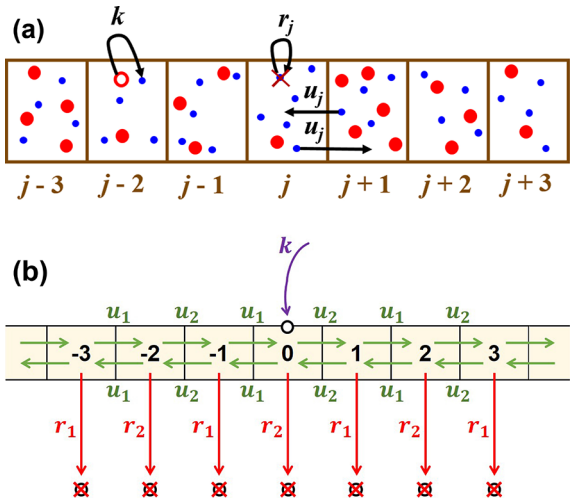

Figure 1. (a) Schematic description of a heterogeneous single nanorod where chemical reactions are catalyzed at active sites (red-filled circles), creating charged holes (blue circles). The nanorod is divided into multiple segments of equal length. A new charged hole appears with the rate k at a given active site (empty red circle). Charged holes can migrate out of segment j to segment $j + 1$ or back from segment $j + 1$ to segment j with the rate u_j, and they can also disappear from segment j with the rate r_j. (b) A simplest alternating heterogeneous discrete-state stochastic model for catalytic communications in a single nanoparticle. There are two types of segments in the system. A new hole is produced at $n = 0$ with a rate k. The forward rate from the odd-numbered segment to the even-numbered segment and the backward rate for the same transition are equal to u_1. Similarly, the forward rate from the even-numbered segment to the odd-numbered segment and the backward rate for the same transition are equal to u_2. The death rate of the charged hole from an odd-numbered (even-numbered) segment is r_1 (r_2).

segment j to segment $j + 1$, as well as the rate to move from segment $j + 1$ to segment j are equal to u_j: see Figure 1a. The charged holes can also disappear with a death rate r_j from segment j. Different position-dependent transition rates reflect the fact that due to structural inhomogeneities, each segment of the nanorod might have a different number of active sites and defects, leading to different migration rates u_j and death rates r_j. Now, a heterogeneous discrete-state stochastic model for catalytic communications can be easily developed as a generalization of the original homogeneous approach.[28] In this model, the average time for the created charged hole to stay in the system corresponds to the communication lifetime, while the average distance that this charged hole moves after creation and before disappearing is associated with the communication length scale.

To better understand the quantitative effects of heterogeneity on catalytic communications, let us consider in detail the simplest heterogeneous model with alternating transition rates, as illustrated in Figure 1b. It is assumed that a new hole is produced on the nanorod with rate k at the segment labeled as state $n = 0$. From this segment, the hole can diffuse to adjacent segments ($n = \pm 1, \pm 2, ...$), and it might also eventually disappear.[28] Additionally, it is assumed that the nanorods are very long. In this approach, the forward transition rates from the odd-numbered segment to the even-numbered segment and the backward transition rates from the even-numbered segment to the odd-numbered segment are given by u_1, while the forward transition rates from the even-numbered segment to the odd-numbered segment and the backward

https://doi.org/10.1021/acs.jpclett.3c01874
J. Phys. Chem. Lett. 2023, 14, 8227−8234

transition rates from the odd-numbered segment to the even-numbered segment are given by u_2: see Figure 1b. In addition, charged holes might disappear from the odd-numbered segments with the rate r_1, while the death rate from the even-numbered segments is r_2. Since all charged holes in the system are independent of each other, in our theoretical framework, we can monitor the evolution of a single hole, and this should provide us with a quantitative description of catalytic communications.

To quantify the catalytic communications in the heterogeneous model with alternating transition rates, we define $P_n(t)$ as the probability of finding a charged hole particle in segment n at time t. Additionally, the function $P_{off}(t)$ describes the probability of the state when the hole has already disappeared and not yet produced on the nanorod. The temporal evolution of these probabilities is described by a set of forward master equations,

$$\frac{dP_n(t)}{dt} = u_1P_{n+1}(t) + u_2P_{n-1}(t) - (u_1 + u_2 + r_1)P_n(t) \tag{1}$$

for odd n, while for even n, we have

$$\frac{dP_n(t)}{dt} = u_2P_{n+1}(t) + u_1P_{n-1}(t) - (u_1 + u_2 + r_2)P_n(t) \tag{2}$$

At the segment where the charged hole is created ($n = 0$), the corresponding expression is

$$\frac{dP_0(t)}{dt} = kP_{off}(t) + u_2P_1(t) + u_1P_{-1}(t) - (u_1 + u_2 + r_2)P_0(t) \tag{3}$$

In addition, for the state of the system when the hole is not present on the lattice (n = off),

$$\frac{dP_{off}(t)}{dt} = r_1\Sigma_{i=odd}P_i(t) + r_2\Sigma_{i=even}P_i(t) - kP_{off}(t) \tag{4}$$

Moreover, there is a normalization condition, requiring that

$$P_{off}(t) + \Sigma_{i=odd}P_i(t) + \Sigma_{i=even}P_i(t) = 1 \tag{5}$$

It is reasonable to assume that the system will quickly reach the steady state after the charged hole is created at $n = 0$,[28] and then one can analytically calculate stationary properties of the system. As explained in detail in the Supporting Information (SI), the stationary probabilities to find the charged hole at the segment n of the nanorod can be written as

$$P_n \simeq By^{|n|}, \quad n = 0, \pm1, \pm2, ... \tag{6}$$

where

$$y = \sqrt{\frac{z}{2u_1u_2} - \sqrt{\left(\frac{z}{2u_1u_2}\right)^2 - 1}} \tag{7}$$

and

$$z = 2u_1u_2 + r_1r_2 + (u_1 + u_2)(r_1 + r_2) \tag{8}$$

The parameters B in eq 6 differ for odd-numbered and even-numbered segments, and they are explicitly evaluated in the SI.

The results of calculations for stationary probabilities (obtained analytically and via Monte Carlo computer simulations) for different heterogeneous situations are listed in Figure 2. One can see that, although alternating transition

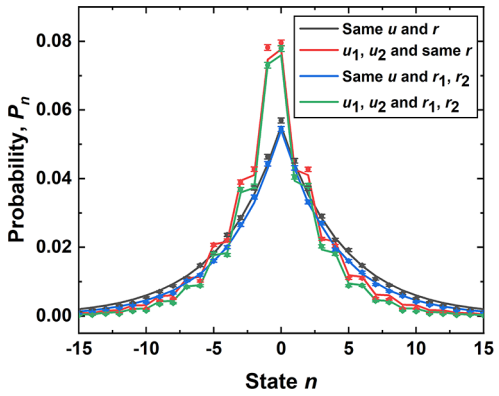

Figure 2. Stationary probability distributions of finding a charged hole at different segments on the nanorod after it is initially produced at segment $n = 0$. The nanorod is assumed to be divided into segments of length $l = 50$ nm. The following parameters have also been used in calculations: $u_1 = 4u$, $u_2 = u/4$, $r_1 = r/2$, $r_2 = 2r$, $k = r = 0.03636$ s^{-1}, and $u = 0.736$ s^{-1}. Solid curves represent the analytical results (assuming infinitely long nanorods), while the symbols correspond to the results from Monte Carlo computer simulations (with the nanorod having a total length of 2550 nm).

rates clearly influence the stationary probabilities, overall these quantities can be viewed as effectively decaying with the distance from the production site at segment $n = 0$. The spread of the distribution describes the region across which the hole is likely to exist before it disappears from the nanorod. Then, the effective characteristic length of this exponential decay (l is the size of each segment),

$$\lambda = -\frac{l}{\ln y} \tag{9}$$

can be associated with the communication lengths in catalytic cooperativity.[28] This is because this length describes the region of increased local concentration due to the produced charged holes, and this increased concentration of charged holes leads to a higher probability of the reaction occurring for the active sites within this region. This exactly corresponds to the correlation length as was measured in experiments.[19] The results of analytical calculations and estimates from Monte Carlo simulations of communication lengths for different heterogeneous cases are also presented in Table 1. It is important to note that this communication length is independent of the hole creation rate, k and is controlled only by the balance between the migration and death rates until it disappears from the lattice. As shown in Figure S1 in the Supporting Information, the rate k affects the amplitude (maximum value) of the distribution whereas the decay region of this distribution remains almost unaltered.

With our theoretical approach, we can estimate the lifetimes τ of the catalytic communication phenomena. This is the time after the new charged hole has been created at the given site by the chemical reaction until it disappears. This leads to

$$\frac{1}{\tau} = \frac{\sum_{j\neq off} r_jP_j}{\sum_{j\neq off} P_j} = \frac{kP_{off}}{1 - P_{off}} \tag{10}$$

This expression reflects the fact that the lifetime can be estimated only when the charged hole is on the nanorod, and it is given by the inverse flux for the charged holes to be removed from the lattice. After substituting the expression of P_{off} from

https://doi.org/10.1021/acs.jpclett.3c01874
J. Phys. Chem. Lett. 2023, 14, 8227−8234

Table 1. Analytically Calculated and Computer Simulation Results of Catalytic Communication Lifetimes (τ) and Distances (λ)[a]

	temporal memory, τ (s)		communication distance, λ (nm)	
case	theory	simulations	theory	simulations
same u and r	27.5 (27.5 ± 2.4)[a]	27.50 ± 0.27	224.96 (225 ± 20)[a]	223.96 ± 2.21
u_1, u_2 and same r	27.5	27.07 ± 0.27	154.32	153.54 ± 1.53
same u and r_1, r_2	22	21.76 ± 0.22	201.21	197.06 ± 1.99
u_1, u_2 and r_1, r_2	22	21.91 ± 0.22	138.03	133.60 ± 1.44

[a]The nanorod is assumed to be divided into segments of length l = 50 nm. The following parameters have been used in calculations: $k = r = 0.03636\ s^{-1}$, $u = 0.736\ s^{-1}$, $\alpha_u = 4$, and $\alpha_r = 2$. The simulation procedure is explained in the Supporting Information. The data in brackets are taken from ref 19 corresponding to the experimentally measured ranges for catalytic communications on Pd nanorods.

eq (S.9c) of the Supporting Information (SI) in eq 10 in this work, it is found that $\tau = M_2/M_1$. These constants M_1 and M_2 are defined in eq (S.8) of the SI and they are independent of the creation rate of the hole k. Thus, the mean lifetime of the hole is not dependent on its creation rate. At the same time, because the lifetimes are independent of the creating rate k, one can propose a simpler two-state model to evaluate this quantity, as explained in the SI. It is shown here that

$$\tau \approx \frac{2u + r_1 + r_2}{u(r_1 + r_2) + 2r_1r_2} \tag{11}$$

This is an excellent approximation to the exact expression for the lifetime, and the reason it is an approximation is that the symmetry of our original model (with the production at the specific site) is slightly different from the simplified two-state model. Also, in the system with the homogeneous death rates, $r_1 = r_2 = r$, we obtain $\tau = 1/r$, in agreement with previous theoretical evaluations of catalytic communications for homogeneous systems.[28]

The lifetime of the catalytic cooperativity is an important factor that affects catalytic processes in the system. If these lifetimes are very short (fast death rates), which corresponds to r_1 and r_2 being much larger than u_1 and u_2, one can obtain from eqs 7 and 8,

$$y \approx \sqrt{\frac{u_1u_2}{r_1r_2}} \tag{12}$$

which leads to the following estimate of the communication length,

$$\lambda \approx \frac{l}{\ln\left(\sqrt{\frac{r_1r_2}{u_1u_2}}\right)} \to 0 \tag{13}$$

Since $r_1, r_2 \gg u_1$, and u_2, these communication lengths are too short to support meaningful catalytic cooperativity at long distances. However, the analysis of experimental measurements suggests that probably a more realistic situation is when the diffusion rates are much faster than the death rates ($u_1, u_2 \gg r_1, r_2$).[28] In this limit, the properties of catalytic communications can be described as

$$\tau \simeq \frac{2}{r_1 + r_2} \tag{14}$$

and

$$\lambda \simeq 2l\sqrt{\frac{u_1u_2}{(r_1 + r_2)(u_1 + u_2)}} \tag{15}$$

Now, considering this realistic case of fast migration rates, it is convenient to quantify the effect of heterogeneity. To do so, let us introduce heterogeneity parameters α_u and α_r via the corresponding expressions for the migration and death rates:

$$u_1 = \alpha_u u, \quad u_2 = \frac{u}{\alpha_u}; \quad r_1 = \alpha_r r, \quad r_2 = \frac{r}{\alpha_r} \tag{16}$$

where rates u and r correspond to the purely homogeneous case. This is a convenient approach, because, by tuning the dimensionless control parameters α_u and α_r, the system can be modified from the homogeneous case ($\alpha_u = \alpha_r = 1$) to any degree of heterogeneity. Please note that this is not a unique way of quantifying heterogeneity, but it can be shown explicitly that the main physics will not change for other scenarios of random distributions of transition rates.

The expressions for the lifetimes and communication distances can now be written as

$$\tau = \frac{1}{r}\frac{2\alpha_r}{\alpha_r^2 + 1} \tag{17}$$

and

$$\lambda = 2l\sqrt{\frac{u}{r}}\sqrt{\frac{\alpha_u\alpha_r}{(1 + \alpha_u^2)(1 + \alpha_r^2)}} \tag{18}$$

In Table 1, we calculated these properties of catalytic cooperativity for alternating heterogeneous models for different distributions of transition rates. One can see that temporal memory (τ) depends only on heterogeneity in the death rates (α_r), but not on the inhomogeneity in the migration rates (α_u). Also, the lifetimes are shorter than those of homogeneous systems. At the same time, communication lengths (λ) depend on both heterogeneity parameters, and they also decrease for more inhomogeneous systems, although the effect is stronger for varying α_u.

To better illustrate the effect of heterogeneity, we introduce dimensionless parameters

$$R(\tau) = \frac{\tau(\alpha_r)}{\tau(\alpha_r = 1)} = \frac{2\alpha_r}{1 + \alpha_r^2} \tag{19}$$

and

$$R(\lambda) = \frac{\lambda(\alpha_r, \alpha_u)}{\lambda(\alpha_r = \alpha_u = 1)} = 2\sqrt{\frac{\alpha_u\alpha_r}{(1 + \alpha_u^2)(1 + \alpha_r^2)}} \tag{20}$$

These quantities specify how the properties of catalytic communications change for heterogeneous systems in comparison to homogeneous systems. The results for specific

https://doi.org/10.1021/acs.jpclett.3c01874
J. Phys. Chem. Lett. 2023, 14, 8227−8234

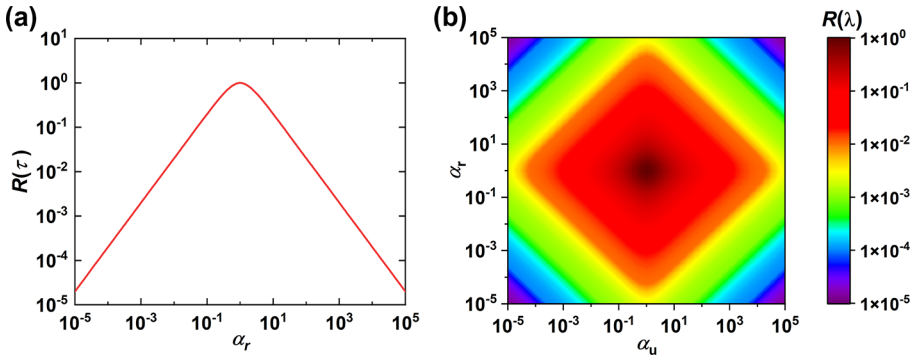

Figure 3. (a) Relative communication lifetimes $R(\tau)$ (see eq 18) as a function of the heterogeneity parameter α_r; and (b) relative communication distances $R(\lambda)$ (see eq 19) as a function of heterogeneity parameters α_u and α_r.

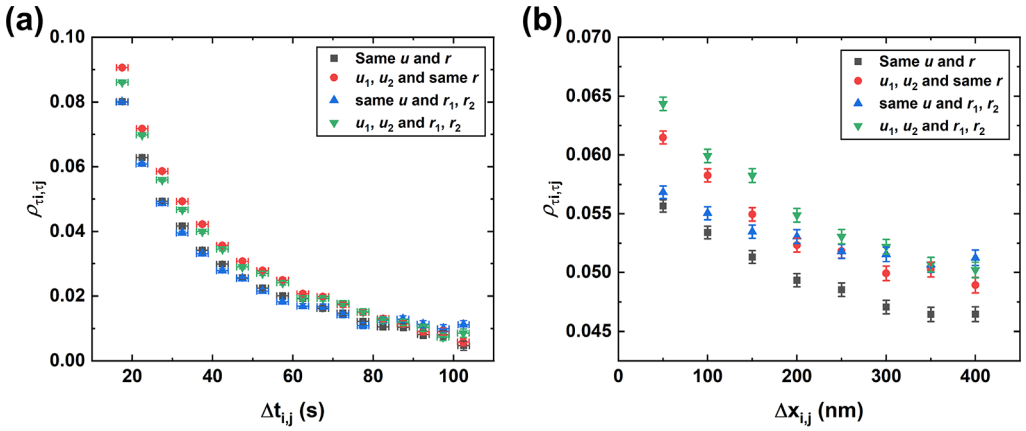

Figure 4. Pearson's cross-correlation coefficients (PCCs) as a function of (a) average time separation, $\Delta t_{i,j}$; and as a function of (b) average distance separation, $\Delta x_{i,j}$, for any segments i and j on the single nanorod. A 1200 nm nanorod is utilized in computer simulations, and it is divided into segments of length l = 50 nm. The following parameters have been also used in calculations: $k = r = 0.03636\ s^{-1}$, $u = 0.736\ s^{-1}$, $\alpha_u = 4$ and $\alpha_r = 2$. The detailed procedure to determine PCCs from Monte Carlo computer simulations is presented in the SI.

calculations for these ratios are presented in Figure 3. As one can see, the longest communication lifetimes and distances can be achieved only for homogeneous systems, and increasing the degree of heterogeneity will always lead to shorter communication lifetimes and distances. Thus, heterogeneity reduces the range of catalytic cooperativity in both spatial and temporal domains.

The effect of inhomogeneous transition rates can also be seen in the stationary probabilities of finding the charged hole at different segments, as illustrated in Figure 2. Modifying the originally homogeneous model ($u_1 = u_2$, $r_1 = r_2$, black curve) by adding heterogeneity only to the death rates ($u_1 = u_2$, $r_1 \neq r_2$, blue curve) changes the distribution P_n only slightly, but one can already see a narrower distribution for the stationary probabilities. However, adding heterogeneity to the migration rates ($u_1 \neq u_2$, $r_1 = r_2$, red curve; and $u_1 \neq u_2$, $r_1 \neq r_2$, green curve) has a much stronger effect: it increases the probability in the region near the origin and makes the whole distribution more narrow further away from the origin (see Figure 2). This actually means that heterogeneity decreases the catalytic communication length, because the region of the increased local concentration of charged holes is now smaller in comparison with the homogeneous system. Additionally, the steady-state distributions become asymmetric on introducing inhomogeneous migration rates. By interchanging the values of the rates u_1 and u_2 (see Figure S2 in the SI), the asymmetry shifts to the opposite direction and it is concluded that slow migration rates from any segment n causes the hole to stay on that segment longer, which increases its probability P_n.

There is another way to evaluate the properties of the catalytic communications. In single-molecule experiments, these properties have been determined by analyzing Pearson's cross-correlation coefficient (PCC or ρ_{τ_i,τ_j}).[19] This quantity exhibited an exponential decay with respect to the average time separation ($\Delta t_{i,j}$) between successive product formation events, as well as the distance separation ($\Delta x_{i,j}$) of any two segments i and j on the single nanorod. The respective decay constants correspond to catalytic communications lifetimes and distances, respectively. In our theoretical approach, we use Monte Carlo computer simulations to mimic experimental measurements, allowing us to evaluate the PCC values. The estimates for the communication lifetimes and distances obtained from these computer simulations are shown in Figure 4. It is found that the amplitude of correlations is larger for the systems with inhomogeneous transition rates in comparison with the homogeneous situations, in agreement with our previous findings.

It is important to emphasize that our theoretical analysis of the role heterogeneity in catalytic communications on single nanorods has concentrated so far on the simplest model with alternating migration and death rates (see Figure 1b). However, it is much more realistic to encounter more random distributions of transition rates in nanoparticles. This situation is illustrated in Figure 5a. In addition, our analysis of the

https://doi.org/10.1021/acs.jpclett.3c01874
J. Phys. Chem. Lett. 2023, 14, 8227−8234

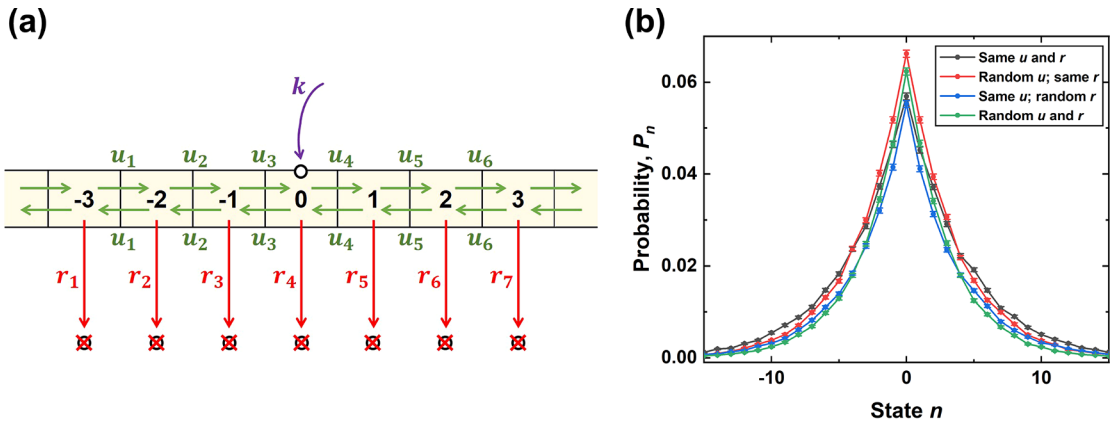

Figure 5. (a) Distinct-state stochastic model of catalytic communications with random transition rates. A new hole is produced at $n = 0$ with a rate k and it diffuses on the nanorod with random migration rates u_i ($i = 1, 2, ...$) until it disappears with a death rate r_i ($i = 1, 2, ...$). (b) Monte Carlo computer simulation results for the steady-state probability distributions of finding a hole at different segments of the nanorod after it is initially produced at segment $n = 0$. All transition rates are randomly chosen from respective Gaussian distributions with the average values of death rates $r = 0.03636\ s^{-1}$ and migration rates $u = 0.736\ s^{-1}$. The nanorod is assumed to be divided into segments of length $l = 50$ nm, and the hole is created with the rate $k = 0.03636\ s^{-1}$.

alternating model suggests that heterogeneity increases the strength of catalytic cooperativity while shortening the communication lengths and lifetimes. But it is unclear if this is a general result or specific to the alternating rates model. To test our theoretical predictions, we now consider a model in which all transition rates are random. More specifically, using Monte Carlo computer simulations, the catalytic communication phenomenon is analyzed for the situations when each rate is taken from different Gaussian distributions. In Figure 5b and Table 2, we present our simulation results for stationary probabilities of created charged holes and for corresponding communication lifetimes and distances. One can again observe that heterogeneity increases the amplitude of catalytic cooperativity near the site where the charged holes are produced. It also leads to decreased communication lifetimes and distances. These results fully agree with our explicit calculations for the alternating heterogeneous models.

Table 2. Catalytic Communications Lifetimes (τ) and Distances (λ) Determined from Monte Carlo Computer Simulations with Random Transition Rates[a]

case	temporal memory, τ (s)	communication distance, λ (nm)
same u and r	27.50 ± 0.27	223.96 ± 2.21
random u and same r	27.47 ± 0.27	186.34 ± 1.86
same u and random r	18.76 ± 0.19	182.46 ± 1.87
random u and r	18.87 ± 0.20	160.98 ± 1.62

[a]All transition rates are randomly chosen from respective Gaussian distributions with the average value of death rates $r = 0.03636\ s^{-1}$ and migration rates $u = 0.736\ s^{-1}$. Furthermore, the standard deviations from the mean values are $\sigma_r = 0.05\ s^{-1}$ and $\sigma_u = 0.5\ s^{-1}$, respectively. The creation rate of a hole is considered to be $k = 0.03636\ s^{-1}$.

Our theoretical analysis that explored analytical calculations and computer simulations indicates that, generally, heterogeneity in transition rates influences catalytic communications by increasing the amplitude of correlations and decreasing the communication lifetimes and distances, as compared to the homogeneous distribution of transition rates. The advantage of our theoretical method is that one can present microscopic arguments to explain these observations.

Let us first compare the properties of catalytic communications for a heterogeneous system with some random distributions of death rates r_j and migration rates u_j in comparison with those of a homogeneous system with uniform averaged death rates $r = \langle r_j \rangle$ and averaged migration rates $u = \langle u_j \rangle$. Charged holes can disappear from any segment of the nanorod, yielding the following death flux:

$$J_{\text{death}} \simeq \sum_j r_j P_j \tag{21}$$

However, this flux is dominated by death events from the segments with the fastest death rates $r_{\max}$. This means that the corresponding communication lifetime, $\tau_{\text{hetero}} = 1/J_{\text{death}} \approx 1/r_{\max}$ is shorter than the corresponding time for the homogeneous system, $\tau_{\text{homo}} = 1/r$ because $r_{\max} \geq r$. Thus, we generally expect to have $\tau_{\text{hetero}} \leq \tau_{\text{homo}}$.

For the diffusion of charged holes along the nanorod, it is expected that they will be found preferentially at the segments with the smallest migration rates, $u_{\min}$, out of them. Then, the average communication distance can be well approximated by $\lambda_{\text{hetero}} \approx \sqrt{\frac{u_{\min}}{r}}$.[28] But this should lead to shorter communication distances than for the homogeneous system, $\lambda_{\text{homo}} \approx \sqrt{\frac{u}{r}}$, since generally we have $u_{\min} \leq u$. Now, because in the heterogeneous model the charged holes after the creation at the given site, on average, will diffuse shorter distances, there will be an increased local concentration of charged holes, which is larger than for the corresponding homogeneous case. This should lead to stronger catalytic cooperativity at these shorter distances since more charged holes are available to stimulate chemical reactions at neighboring active sites. The results of our theoretical calculations and computer simulations are fully consistent with these more microscopic arguments.

We presented a theoretical investigation of the role of heterogeneity in catalytic communication phenomena on single nanoparticles. Because of the variability of structural properties of nanocatalysts, in our theoretical approach, the heterogeneity is accounted for by considering random distributions of transition rates of charged holes that control catalytic cooperativity. To reflect experimental observations of catalytic processes on nanorods, an analysis is done for

https://doi.org/10.1021/acs.jpclett.3c01874
J. Phys. Chem. Lett. 2023, 14, 8227−8234

effective 1D systems. This allows us to extend the original homogeneous discrete-state stochastic model to situations with inhomogeneous diffusion and death rates for charged holes. By specifically considering a simplified heterogeneous model, where transition rates alternate between odd and even segments of the nanorod, we evaluate the properties of catalytic communications phenomena via exact analytical calculations supplemented by Monte Carlo simulations. It is found that heterogeneity generally decreases the catalytic communication lifetimes and distances, although the effect of cooperativity becomes stronger. Similar trends have also been observed for general models with random distributions of transition rates, supporting the generality of our theoretical predictions on the nature of heterogeneity in catalytic communications. Furthermore, microscopic arguments to explain these observations have also been also presented. Our theoretical results suggest that specific details of local structures around the active sites (facet types, roughness, defects, etc.) might be the leading factors that can be tuned to control the efficiency of catalytic processes at these sites.

It is important to critically evaluate our theoretical approach. To model the variability of chemical and structural properties of single nanocatalysts, a specific "bond" heterogeneity has been assumed in our theoretical method. In other words, for the specific bond that connects two neighboring segments of the nanorod, we assumed the same migration rates, while these rates are different for other bonds. However, there is another scenario of how heterogeneity might be implemented, which we label as a "segment" heterogeneity. In this case, one could assume the migration rates in any direction from the given segment to be the same and the corresponding diffusion rates are different for other segments. We expect that the quantitative values of the catalytic communication properties will depend on different heterogeneity scenarios, but the general trends (increased correlation strength, decreased communication lifetimes, and distances) will be the same. In addition, it was assumed that stationary dynamics is quickly reached in the system, but this might not be the case. Thus, it will be interesting to investigate transient phenomena in catalytic communication processes.

Also, in our theoretical method, we postulated that catalyzed chemical reactions produce charged holes and that the probability for the active site to operate depends on the local concentration of holes. These statements, although plausible, have not been experimentally tested. In addition, although nanorods are three-dimensional (3D) systems, a minimal 1D description is sufficient to quantitatively probe catalytic cooperative communications within single nanorods. However, this 1D description is valid only for nanorods, and for more complex nanoparticles (such as nanoplates), a 2D description may be explored. Furthermore, infinitely long nanorods have been assumed in our analytical calculations, but the real nanoparticles are finite, and some finite-size effects might be present. Finally, although there are currently no experimental observations, the advantage of our method is that there are specific predictions, at least for general trends in catalytic communications, that can be utilized to probe our theoretical predictions. This should lead to a better understanding of the fundamental mechanisms of catalytic processes.

■ ASSOCIATED CONTENT

Supporting Information

The Supporting Information is available free of charge at https://pubs.acs.org/doi/10.1021/acs.jpclett.3c01874.

Calculations to determine steady-state probabilities and details of Monte Carlo computer simulations (PDF)

■ AUTHOR INFORMATION

Corresponding Authors

Srabanti Chaudhury − *Department of Chemistry, Indian Institute of Science Education and Research, Pune 411008 Maharashtra, India;* orcid.org/0000-0001-6718-8886; Email: srabanti@iiserpune.ac.in

Anatoly Kolomeisky − *Department of Chemistry, Department of Chemical and Biomolecular Engineering, Department of Physics and Astronomy, and Center for Theoretical Biological Physics, Rice University, Houston, Texas 77005, United States;* orcid.org/0000-0001-5677-6690; Email: tolya@rice.edu

Author

Bhawakshi Punia − *Department of Chemistry, Indian Institute of Science Education and Research, Pune 411008 Maharashtra, India*

Complete contact information is available at: https://pubs.acs.org/10.1021/acs.jpclett.3c01874

Author Contributions

[▽]These authors contributed equally to this work.

Notes

The authors declare no competing financial interest.

■ ACKNOWLEDGMENTS

B.P. thanks IISER Pune and the Prime Minister Research Fellowship (PMRF), India, for funding and fellowship. S.C. acknowledges support from SERB, India (No. SPF/2022/000155 and CRG/2019/000515). A.B.K. acknowledges the support from the Welch Foundation (No. C-1559), from the NSF (Nos. CHE-1953453 and CHE-2246878), and by the Center for Theoretical Biological Physics sponsored by the NSF (No. PHY-2019745).

■ REFERENCES

(1) Farrauto, R.; Dorazio, L.; Bartholomew, C. *Introduction to Catalysis and Industrial Catalytic Processes*; Wiley, 2016.
(2) Somorjai, G.; Li, Y. *Introduction to Surface Chemistry and Catalysis*; Wiley, 2010.
(3) Roduner, E. Understanding catalysis. *Chem. Soc. Rev.* **2014**, *43*, 8226−8239.
(4) Ross, J.. *Heterogeneous Catalysis: Fundamentals and Applications*; Elsevier, 2011.
(5) Fechete, I.; Wang, Y.; Védrine, J. C. The past, present and future of heterogeneous catalysis. *Catal. Today* **2012**, *189*, 2−27.
(6) Schlögl, R. Heterogeneous catalysis. *Angew. Chem., Int. Ed.* **2015**, *54*, 3465−3520.
(7) Liu, L.; Corma, A. Metal catalysts for heterogeneous catalysis: from single atoms to nanoclusters and nanoparticles. *Chem. Rev.* **2018**, *118*, 4981−5079.
(8) Astruc, D. Introduction: Nanoparticles in catalysis. *Chem. Rev.* **2020**, *120*, 461−463.
(9) Tao, F.; Spivey, J. *Metal Nanoparticles for Catalysis: Advances and Applications*; Royal Society of Chemistry, London, 2014.

(10) Roldan Cuenya, B. Metal nanoparticle catalysts beginning to shape-up. *Acc. Chem. Res.* **2013**, *46*, 1682−1691.
(11) An, K.; Somorjai, G. A. Size and shape control of metal nanoparticles for reaction selectivity in catalysis. *ChemCatChem.* **2012**, *4*, 1512−1524.
(12) Janssen, K. P.; De Cremer, G.; Neely, R. K.; Kubarev, A. V.; Van Loon, J.; Martens, J. A.; De Vos, D. E.; Roeffaers, M. B.; Hofkens, J. Single molecule methods for the study of catalysis: from enzymes to heterogeneous catalysts. *Chem. Soc. Rev.* **2014**, *43*, 990−1006.
(13) Decan, M. R.; Impellizzeri, S.; Marin, M. L.; Scaiano, J. C. Copper nanoparticle heterogeneous catalytic 'click' cycloaddition confirmed by single-molecule spectroscopy. *Nat. Commun.* **2014**, *5*, 1−8.
(14) Shen, H.; Zhou, X.; Zou, N.; Chen, P. Single-molecule kinetics reveals a hidden surface reaction intermediate in single-nanoparticle catalysis. *J. Phys. Chem. C* **2014**, *118*, 26902−26911.
(15) Sambur, J. B.; Chen, P. Approaches to single-nanoparticle catalysis. *Annu. Rev. Phys. Chem.* **2014**, *65*, 395−422.
(16) Chen, T.; Zhang, Y.; Xu, W. Single-molecule nanocatalysis reveals catalytic activation energy of single nanocatalysts. *J. Am. Chem. Soc.* **2016**, *138*, 12414−12421.
(17) Qu, X.; Zhao, B.; Zhang, W.; Zou, J.; Wang, Z.; Zhang, Y.; Niu, L. Single-Molecule Nanocatalysis Reveals the Kinetics of the Synergistic Effect Based on Single-AuAg Bimetal Nanocatalysts. *J. Phys. Chem. Lett.* **2022**, *13*, 830−837.
(18) Chen, P.; Zhou, X.; Andoy, N. M.; Han, K.-S.; Choudhary, E.; Zou, N.; Chen, G.; Shen, H. Spatiotemporal catalytic dynamics within single nanocatalysts revealed by single-molecule microscopy. *Chem. Soc. Rev.* **2014**, *43*, 1107−1117.
(19) Zou, N.; Zhou, X.; Chen, G.; Andoy, N. M.; Jung, W.; Liu, G.; Chen, P. Cooperative communication within and between single nanocatalysts. *Nat. Chem.* **2018**, *10*, 607−614.
(20) Xu, W.; Kong, J. S.; Yeh, Y.-T. E.; Chen, P. Single-molecule nanocatalysis reveals heterogeneous reaction pathways and catalytic dynamics. *Nat. Mater.* **2008**, *7*, 992−996.
(21) Zhou, X.; Xu, W.; Liu, G.; Panda, D.; Chen, P. Size-dependent catalytic activity and dynamics of gold nanoparticles at the single-molecule level. *J. Am. Chem. Soc.* **2010**, *132*, 138−146.
(22) Zhang, Y.; Song, P.; Chen, T.; Liu, X.; Chen, T.; Wu, Z.; Wang, Y.; Xie, J.; Xu, W. Unique size-dependent nanocatalysis revealed at the single atomically precise gold cluster level. *Proc. Natl. Acad. Sci. U.S.A.* **2018**, *115*, 10588−10593.
(23) Lee, K.; Kim, M.; Kim, H. Catalytic nanoparticles being facet-controlled. *J. Mater. Chem. A* **2010**, *20*, 3791−3798.
(24) Chen, T.; Chen, S.; Song, P.; Zhang, Y.; Su, H.; Xu, W.; Zeng, J. Single-molecule nanocatalysis reveals facet-dependent catalytic kinetics and dynamics of pallidium nanoparticles. *ACS Catal.* **2017**, *7*, 2967−2972.
(25) Tachikawa, T.; Yamashita, S.; Majima, T. Evidence for crystal-face-dependent TiO2 photocatalysis from single-molecule imaging and kinetic analysis. *J. Am. Chem. Soc.* **2011**, *133*, 7197−7204.
(26) Zhou, X.; Andoy, N. M.; Liu, G.; Choudhary, E.; Han, K.-S.; Shen, H.; Chen, P. Quantitative super-resolution imaging uncovers reactivity patterns on single nanocatalysts. *Nat. Nanotechnol.* **2012**, *7*, 237−241.
(27) Andoy, N. M.; Zhou, X.; Choudhary, E.; Shen, H.; Liu, G.; Chen, P. Single-molecule catalysis mapping quantifies site-specific activity and uncovers radial activity gradient on single 2D nanocrystals. *J. Am. Chem. Soc.* **2013**, *135*, 1845−1852.
(28) Punia, B.; Chaudhury, S.; Kolomeisky, A. B. Microscopic mechanisms of cooperative communications within single nanocatalysts. *Proc. Natl. Acad. Sci. U.S.A.* **2022**, *119*, No. e2115135119.
(29) Furube, A.; Asahi, T.; Masuhara, H.; Yamashita, H.; Anpo, M. Charge carrier dynamics of standard TiO2 catalysts revealed by femtosecond diffuse reflectance spectroscopy. *J. Phys. Chem. B* **1999**, *103*, 3120−3127.
(30) Studer, A.; Curran, D. P. The electron is a catalyst. *Nat. Chem.* **2014**, *6*, 765−773.
(31) Hu, Q.; Yu, X.; Gong, S.; Chen, X. Nanomaterial catalysts for organic photoredox catalysis-mechanistic perspective. *Nanoscale* **2021**, *13*, 18044−18053.
(32) Xu, W.; Kong, J. S.; Chen, P. Probing the catalytic activity and heterogeneity of Au-nanoparticles at the single-molecule level. *Phys. Chem. Chem. Phys.* **2009**, *11*, 2767−2778.
(33) Chaudhury, S.; Jangid, P.; Kolomeisky, A. B. Dynamics of chemical reactions on single nanocatalysts with heterogeneous active sites. *J. Chem. Phys.* **2023**, *158*, 074101.

https://doi.org/10.1021/acs.jpclett.3c01874
J. Phys. Chem. Lett. 2023, 14, 8227−8234